ROBUST CONTROL FOR HAPTIC-BASED ROBOTIC TELEOPERATION

ALEŠ HACE[1], MARKO FRANC[2]

Abstract. The paper deals with teleoperated robotic systems that are commanded by a human operator via interface that provides task feedback information. In order to successfully perform challenging tasks, not only visual, but also a haptic feedback is strongly desired. Thus, such teleoperator system has to be controlled bilaterally. The paper presents a bilateral control scheme which is designed based on modal decomposition to decouple force and position coordinates. The control algorithm is derived following the sliding mode control approach which guarantees robustness to model perturbation, parameters uncertainty and system disturbance. The proposed design also applies external force observer; thus, none external force sensor is required. The design was experimentally validated on a simple master-slave teleoperator with a 1-DoF robotic system.

Key words: bilateral control, master-slave robot system, force sensation, sliding mode control, force reflection.

1. INTRODUCTION

Telerobotics [1] provides the human operator the possibility to perform tasks in the remote environment. It the past, it has been introduced mainly at applications where a human operator cannot be physically present or access the object concerned in the robotic task. Beside traditional applications which comprise handling in hazardous or inaccessible environments as space, underwater, nuclear plants many other uses of advanced telerobotic systems have been developed, such as robotic surgery. In these applications the robotic system is operating by a human operator in manual or semiautonomous regime, *i.e.* it is teleoperated via a sort of user interface that can provide task feedback information. Such robotic system can be also called teleoperating system or teleoperator. The teleoperator system comprises master device for command interface and the slave robotic system. The slave robotic system may interact with the environment. For various robotic tasks the performance in the interaction with the environment may be important. The interaction with remote environment can be reproduced by a haptic device that

[1] Institute of Robotics, University of Maribor, Slovenia
[2] Isomat d.o.o., Slovenia

Rom. J. Techn. Sci. – Appl. Mechanics, Vol. 58, Nº 1–2, P. 127–151, Bucharest, 2013

stimulates human kinesthetic sense of a local operator. Then, the interface provides remote contact information to the human operator that can feel remote environment. He or she can conduct tasks more safely and more effectively.

The teleoperating robotic system, which provides advanced task performance in a non-autonomous mode with human operator in the loop, requires not only visual but also a haptic feedback which is more intuitive. The haptic-based interface is utilized to provide motion commands for slave device and to faithfully reproduce remote interaction forces simultaneously. Furthermore, both the master and the slave can be complex robotic systems with multi degree-of-freedoms. A block scheme of the teleoperation system with is depicted by Figure 1. Display of force feedback to the operator can be straightforward in principle; in force-reflecting master-slave teleoperators the measured force signals drive motors on the master robotic device that push back on the hand of the operator to stimulate human kinesthetic sense with the same forces and torques with which the slave pushes on the environment. Such teleoperation system operates in bilateral mode. This might work perfectly in an ideal world where such slave-back-to-master force tracking is perfect, and the master and slave arms impose no mass, compliance, viscosity, or static friction characteristics of their own. However, in reality we must count on all these effects, which consequently make harder or impossible to achieve the ideal teleoperator characteristics.

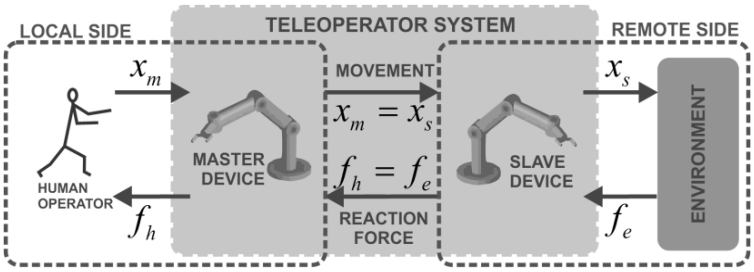

Fig. 1 – Bilateral teleoperation.

A few basic bilateral teleoperation control scheme appeared in past that differs regarding performance and stability [2−4]. However, the bilateral teleoperation control problem still attracts lots of researchers worldwide in order to improve performance, stability and robustness [5−8]. Transparency is one of the performance indices of bilateral teleoperation systems [7]. High transparency means that a force control and a position control are perfectly achieved both in the master side and in the slave side. In fact, the force control and the position control have to be achieved with accuracy to match master and slave the force responses and the position responses, respectively. However, decomposition of a bilateral control system into two components, *i.e.* the force control system and the position

control system, is a problem. These two control modes should be designed independently for ideal bilateral control. For above purpose, some researchers have utilized the paradigm of the disturbance observer (DOB) and the mode decomposition in order to improve performance and robust stability of bilateral teleoperation [9–13].

It has been shown, that sensorless force control is the one of the fundamental techniques for evolution of human-cooperating robot [14]. However, in combination with the acceleration control, robustness may be also significantly improved [13]. On the other side, impedance control offers unified approach for regulation in both position and force coordinate, and thus it may be applied to improve stability while contacting stiff environment. When contact occurs, the arising forces will be dictated by the dynamic interbalancing of the system incorporating the human operator, the master and slave robot and the environment. To assign a prescribed dynamic behavior for the robot while its end-effector is interacting with the environment, the impedance control can be utilized to assure stable contact. It enables for controlling the robot in both free space and constrained motion control. A fundamental work on impedance control was published by [15]. In this work, the complete knowledge of the dynamic model of the robot is necessary to implement computed torque control technique and thus to enforce the desired impedance; however, the teleoperation has not been considered. The impedance control in bilateral telemanipulation has been presented by [16]. Not necessarily, but normally 4-ch teleoperation paradigm (both position or velocity signals and force signals are interchanged) is to be applied in fully impedance control [17]. Impedance control approach has been investigated for use in teleoperation with haptic interface system characterized by parallel robotic mechanism [18]. In [19], the authors focus on transparency and tracking performance improvement of teleoperation system by using an impedance control based on inverse dynamics. In [20] another impedance controller is designed for bilateral teleoperation. The impedance control is based on computed torque or inverse dynamics approach and applied for teleoperation system. The above mentioned approach requires complete knowledge of nonlinear robot model and lacks robustness. However, robust stability of bilateral teleoperation control for force reflection or haptic interface under system uncertainties and disturbances is important to study [15].

Sliding Mode Control (SMC) design approach may be also utilized to further considerably improve robustness in a feedback control [22]. Though switching control was originally introduced to guarantee stability while the system remains constraint to the selected sliding manifold, in mechanical systems in which the control input can only be a continuous function of time, sliding mode controller design can be a challenging task. Impedance control scheme for robot manipulators based on SMC design with continuous control has been introduced in [23]. The proposed control scheme preserves robustness while preventing chattering due to

bang-bang switching control. Due to its robustness SMC design has been implemented also in the problem of bilateral teleoperation [24].

This paper presents a bilateral control algorithm for telerobotic system with a vivid haptic interface. The impedance control design is performed in the virtual modes [13]. Force servoing is achieved in the common mode and position tracking control is provided in the differential mode. Hence, simultaneous force and position control are obtained independently. The derivation of the robust control algorithm is based on sliding mode control design since it allows coping with modeling uncertainties, unknown parameters, and external disturbance that are normally present within the robotic systems. Furthermore, it guarantees high performance tracking control. In order to avoid undesired chattering, derivation of smooth control signal is prioritized. External action/reaction force estimation by force reaction observer was used for experimental validation of the proposed control scheme in place of force sensors. Avoiding the use of strain gauge force sensors provides not only higher force sensing bandwidth but makes the control scheme also proper for applications where the use of sensors is not possible.

The structure of the paper is as follows. In section 2 the problem of bilateral teleoperation is formulated and the control objective in the virtual modes is introduced. Section 3 presents the derivation of the control algorithm for bilateral teleoperation, and section 4 shows experimental results with a short discussion. Section 5 concludes the paper.

2. PROBLEM FORMULATION

The model of a bilateral teleoperation system is depicted by Figure 1. The teleoperator is connected to the human operator on one side by master command device and on the other side may be in contact with environment by slave device. Both master and slave devices are robotic mechanisms.

2.1. ROBOT DYNAMICS

The motion equation for a nonredundant robot dynamics with rotational joints can be written as [25]

$$\mathbf{M}(\mathbf{q})\ddot{\mathbf{q}} + \mathbf{c}(\mathbf{q},\dot{\mathbf{q}}) + \mathbf{g}(\mathbf{q}) = \boldsymbol{\tau} - \mathbf{J}^{\mathrm{T}}\mathbf{f}^{\mathrm{ext}}, \tag{1}$$

where $\mathbf{q}$, $\dot{\mathbf{q}}$, $\ddot{\mathbf{q}}$, and $\boldsymbol{\tau}$ are n-dimensional vectors of joint position, velocity, acceleration and applied motor torque, respectively, and n denotes number of robot degrees-of-freedom. $\mathbf{f}^{\mathrm{ext}}$ is in general a spatial 6D vector and denotes external force acting on the robot end effector due to contact with environment. $\mathbf{M}$ is $n \times n$ symmetric and positive definite matrix, called the joint-space inertia matrix. $\mathbf{c}$ determines effects of Coriolis and centrifugal forces expressed in joint space, $\mathbf{g}$

stands for the effect of gravitational field. The matrix **J** is the Jacobian of the robot end-efector that satisfies equation

$$\dot{\mathbf{x}} = \mathbf{J}(\mathbf{q})\dot{\mathbf{q}}, \tag{2}$$

where $\dot{\mathbf{x}}$ is spatial 6D velocity vector of end effector and the Jacobian can be derived as $\mathbf{J}(\mathbf{q}) = \partial \mathbf{L}(\mathbf{q}) / \partial \mathbf{q}$ where $\mathbf{L}(\mathbf{q})$ denotes geometrical transformation of joint position vector to the task space robot end-effector spatial 6D vector.

$$\mathbf{x} = \mathbf{L}(\mathbf{q}). \tag{3}$$

Furthermore, if one defines spatial 6D acceleration vector

$$\ddot{\mathbf{x}} = \mathbf{J}(\mathbf{q})\ddot{\mathbf{q}} + \dot{\mathbf{J}}(\mathbf{q})\dot{\mathbf{q}}, \tag{4}$$

then the alternative form of robot dynamics can be expressed in the operational-space, i.e. in the robot task-space, which is the space in which the robot is commanded to operate:

$$\mathbf{M}_x(\mathbf{x})\ddot{\mathbf{x}} + \mathbf{c}_x(\mathbf{x}, \dot{\mathbf{x}}) + \mathbf{g}_x(\mathbf{x}) = \mathbf{f} - \mathbf{f}^{\text{ext}}, \tag{5}$$

where the control input is related by motor torques as $\boldsymbol{\tau} = \mathbf{J}^{\mathrm{T}}\mathbf{f}$, $\mathbf{M}_x$ is operational-space mass matrix, $\mathbf{c}_x$ contains Coriolis and centrifugal force terms whereas $\mathbf{g}_x$ contains gravity force terms.

The robot dynamics can be viewed as a set of interconnected SISO systems

$$m_{ii}(\mathbf{x})x_i + \sum_{j=1, j\neq i}^{6} m_{ij}(\mathbf{x})\ddot{x}_j + c_i(\mathbf{x}, \dot{\mathbf{x}}) + g_i(\mathbf{x}) = f_i - f_i^{\text{ext}}, \tag{6}$$

where $i = 1...6$. If one defines the signal that contains system perturbation and external disturbance by

$$d_i = -(\Delta m_{ii}(\mathbf{x})\ddot{x}_i + \sum_{j=1, j\neq i}^{6} m_{ij}(\mathbf{x})\ddot{x}_j + c_i(\mathbf{x}, \dot{\mathbf{x}}) + g_i(\mathbf{x}) + f_i^{\text{ext}}), \tag{7}$$

where $\Delta m_{ij}(\mathbf{x}) = m_{ii}(\mathbf{x}) - \bar{m}_i(x_i)$, and $\bar{m}_i$ is a nominal mass of the *i*-th axis in operational space. Then, the robot dynamics from can be rewritten as

$$\bar{m}_i\ddot{x}_i = f_i - d_i \tag{8}$$

or in the compact form

$$\bar{\mathbf{M}}\ddot{\mathbf{x}} = \mathbf{f} - \mathbf{d}, \tag{9}$$

where $\bar{\mathbf{M}} = \text{diag}(\bar{m}_i)$, $i = 1, ... 6$, is the diagonal nominal mass matrix, $\mathbf{d} = [d_1, ..., d_6]$ is the disturbance vector.

2.2. TRANSPARENCY OPTIMIZED BILATERAL TELEOPERATION

In bilateral teleoperation, information about the task at the remote site is required to help a human operator to feel as they are physically present at the remote place. The teleoperator system consists of master and slave robotic device, each may be described by a simple mode in Cartesian coordinates:

$$Z_m v_m = f_m + f_h, \tag{10}$$

$$Z_s v_s = f_s - f_e, \tag{11}$$

where Z_m, Z_s, v_m, v_s, f_m, f_s are impedance, velocity and control force of master and slave robotic device, respectively. f_h is action force which is generated by human operator while manoeuvring the master device, and f_e is reaction force which appears while slave device is touching remote environment. The operator moves a master device and its velocity v_m is transmitted to the slave device, which is forced to follow the master movement. The ideal motion tracking assumes that the slave will follow the commanded motion at every time instant, *i.e.* $v_s = v_m$. When the slave device contacts the remote environment, the environment reaction force f_e is transmitted back to the human operator who should sense $f_h = f_e$. If operators are to feel as if they are touching the task directly, then the operator's force on the master f_h and the master's motion v_m should have the same relationship, i.e., for the same forces $f_h = f_e$ the same motion is also desired $v_s = v_m$. However, the ideal relation between the signals can be expressed by simple hybrid matrix **h**:

$$\begin{bmatrix} f_h \\ -v_s \end{bmatrix} = \mathbf{h} \begin{bmatrix} v_m \\ f_e \end{bmatrix}, \quad \mathbf{h} = \begin{bmatrix} h_{11} & h_{12} \\ h_{21} & h_{22} \end{bmatrix}. \tag{12}$$

The ideal behavior for a bilateral teleoperation system is to provide a faithful simultaneous transmission of signals between the master and slave to couple the operator as closely as possible to the remote task: i) force matching – the force that human operator applies to the master arm is matched to the force reflected from the environment in the steady state (this can help operators to realize force sensation), ii) kinematically correspondence – the slave position is matched with the master position in the steady state, iii) the teleoperator must remain stable.

If positions, velocities, and forces of the master and slave device are matched, then the values of the hybrid matrix can be written as:

$$\mathbf{h} = \begin{bmatrix} h_{11} & h_{12} \\ h_{21} & h_{22} \end{bmatrix} = \begin{bmatrix} 0 & 1 \\ -1 & 0 \end{bmatrix} \tag{13}$$

and the teleoperator provides complete *transparency* [3]. Transparency is an important performance index in the bilateral teleoperation control scheme design. Ideally, the teleoperation system would be completely transparent, so that operators would feel that they are directly interacting with the remote task. The desired dynamic behavior of the teleoperator is, therefore, close to a rigid rod with minimal inertia and maximal stiffness. Thus, the connection of the master and slave arms should have zero mass and infinite stiffness. When the slave robot performs a contact task, then the slave velocities and forces are not independent. They are related by impedance of the slave environment Z_e. Transparency degree of the teleoperator can be expressed by so called *transmitted impedance* Z_t, that is property of a teleoperator and can be derived from a teleoperator hybrid matrix **h** description as:

$$Z_t = h_{11} - \frac{h_{12}h_{21}}{Z_e^{-1} + h_{22}}. \tag{14}$$

Theoretically, the conditions for perfect transparency $Z_t \equiv Z_e$ when the remote environment is ideally "displayed" to the human operator, can be determined such as: i) $h_{11} = 0$, ii) $h_{22} = 0$, iii) $h_{12}h_{21} = -1$. Furthermore, in order to assure kinematic correspondence, the following condition must also be fulfilled: iv) $h_{21} = -1$ and $h_{12} = 1$. These are same results as suggested by (12)–(13) and present conditions for the *transparency-optimized teleoperator*.

The desired transparency of the bilateral teleoperator can be achieved only if *stability* of the bilateral teleoperation system can be assured. Thus, (robust) stability remains the most important goal in any bilateral controller design. The accurate closed-loop analysis with precise and sufficient condition for stability is extremely difficult to obtain since the system is multivariable in general and dependent on a particular human and environment characteristics. However, one can study stability properties by application of *absolute stability* condition that guarantees stability by assuring passivity of the one-port networks resulted from terminating master-slave two-port network by any passive environment and operator. By Llewellyn's absolute stability criterion one can state that the teleoperator two-port network LTI model (12) will be stable if and only if [2]:

- the hybrid parameters h_{11} and h_{22} have no poles on the right-half plane, and
- any poles of h_{11} and h_{22} on the imaginary axis are simple and have real and positive residues, and

- the inequalities below hold on $j\omega$ axis for all $\omega \geq 0$.

$$\begin{aligned} &\Re\{h_{11}\} \geq 0 \\ \eta_h(\omega) = -\frac{\Re\{h_{12}h_{21}\}}{|h_{12}h_{21}|} + 2\frac{\Re\{h_{11}\}\Re\{h_{22}\}}{|h_{12}h_{21}|} &\geq 1 \end{aligned} \quad . \tag{15}$$

The stability criterion suggests that the transparency-optimized teleoperator can be only marginally stable as $\Re\{h_{11}\} \equiv 1$ and $\eta_h(\omega) \equiv 1$, thus stability is hard to achieve in case of perfect transparency. Transparency and robust stability are obviously conflicting design goals in bilateral teleoperation systems since good transparency usually implies strong coupling from master to slave, and in contrast, the sufficient conditions for stability results in conservative design criteria leading to poor transparency [3]. Thus, bilateral control design will be a compromise between stability and the teleoperator performance.

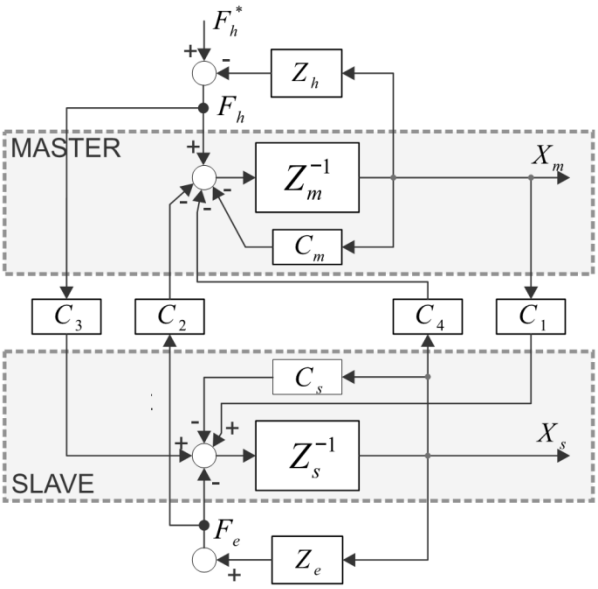

Fig. 2 – 4-channel bilateral control block scheme.

Although few basic control architectures can be designed for master-slave bilateral teleoperation, the 4-channel architecture depicted by Figure 2 is most general [3]. In this case, general multivariable system architecture is utilized which includes all four types of data transmission between master and slave: force and velocity in both directions. The 4-channel architecture requires position and force sensors in both robots, in order to feed data to the four communication channels. It has been shown that a proper use of all four channels is of critical importance in

achieving high performance sense of accurate transmission of remote impedances to the operator. In this algorithm, all the parameters are much coupled and it is not easy to predict how a change in any of them will affect the performance of the system. However, the analytical expressions obtained for this teleoperation control scheme show its capability to achieve perfect position and force tracking with infinite bandwidth – such teleoperator is thus ideally transparent $Z_t = Z_e$. The 4-channel controller seems to be clearly superior to the other algorithms from any point of view. However, in order to achieve perfect transparency, the master and slave dynamics have to be cancelled out simultaneously and the forces fed forward have to match forces exerted by the operator or the environment exactly. Moreover, this selection of parameters requires the evaluation of accelerations that is usually not available in practice and therefore the architecture is hardly to provide necessary robust stability. Thus, acceleration shall be cancelled out from the control signal in *practical* 4-channel architecture and then the master and slave control laws for bilateral teleoperation can be described as follows:

$$f_m = -C_m^p x_m + C_4 x_s + C_m^f f_h - C_2 f_e, \tag{16}$$

$$f_s = -C_s^p x_s + C_4 x_m + C_s^f f_e - C_2 f_h, \tag{17}$$

where x_m, x_s are position of master and slave, respectively, and $\dot{x}_m = v_m$, $\dot{x}_s = v_s$. C_m^p and C_s^p are master and slave local PD position controllers, respectively, C_m^f and C_s^f are master and slave local force P controllers, respectively. The control laws are supplemented by the portions for teleoperation: C_1 and C_4 are channel or remote position controllers, and C_2 and C_3 are channel or remote force controllers. However, removing acceleration from the control feedback signal reasonably impairs performance of the bilateral teleoperator. In order to determine the optimal selection of the local control and channel controllers one can derive the transmitted impedance expression Z_t:

$$Z_t = \frac{(Z_m + C_m^p)(Z_s + C_s^p) - C_1 C_4 + (C_1 C_2 + \bar{C}_s^f (Z_m + C_m^p))Z_e}{\bar{C}_m^f (Z_s + C_s^p) + C_3 C_4 + (\bar{C}_m^f \bar{C}_s^f - C_2 C_3) Z_e}, \tag{18}$$

where $\bar{C}_i^f = 1 + C_i^f$, $i = m, s$ and Z_m, Z_s are master and slave robot impedance, respectively. By selection of the channel controllers such as:

$$\begin{aligned} C_1 &= C_s^p, \quad C_4 = C_m^p, \\ C2 &= \bar{C}_m^f, \quad C_3 = \bar{C}_s^f, \end{aligned} \tag{19}$$

one can obtain

$$Z_t = \frac{Z_m Z_s + Z_m C_s^p + Z_s C_m^p + (\bar{C}_m^f C_s^p + \bar{C}_s^f Z_m + \bar{C}_s^f C_m^p) Z_e}{\bar{C}_m^f C_s^p + \bar{C}_m^f Z_s + \bar{C}_s^f C_m^p}. \tag{20}$$

The local controllers can be tuned such that the relations

$$\frac{C_m^p}{C_s^p} = \frac{\bar{C}_m^f}{\bar{C}_s^f} = \frac{Z_m}{Z_s} \tag{21}$$

imply definitions of *common mode* teleoperator impedance $Z_c = \frac{Z_m}{\bar{C}_m^f} = \frac{Z_s}{\bar{C}_s^f}$ and *differential mode* position controller $C_d^p = \frac{C_m^p}{\bar{C}_m^f} + \frac{C_s^p}{\bar{C}_s^f}$. Such mode transformation decouples the problem of force control and differential position control in bilateral teleoperation. Consequently, the expression for the transmitted impedance (19) can be simplified as:

$$Z_t = Z_c + Z_e. \tag{22}$$

The perfect transparency is not possible to achieve by practical 4-channel architecture since such bilateral control scheme cannot cancel out the teleoperator impedance. However, the common mode impedance can be arbitrary tuned by local force feedback gains. The hybrid matrix for the practical 4-channel teleoperator can be written as:

$$\mathbf{h} = \begin{bmatrix} Z_c & 1 \\ -1 & 0 \end{bmatrix}. \tag{23}$$

Z_c determines the teleoperator impedance in free motion. It is responsible for operationability [26] of the teleoperator.

2.3. DECOMPOSITION OF BILATERAL TELEOPERATION BY THE VIRTUAL MODES

Without loss of generality the teleoperator dynamics from (10) and (11) can be rewritten in the compact form:

$$\mathbf{M}\ddot{\mathbf{x}} = \mathbf{f} + \mathbf{f}^{\text{ext}}, \tag{24}$$

where $\mathbf{x} = [x_m, x_s]^{\mathrm{T}}$, $\mathbf{f} = [f_m, f_s]^{\mathrm{T}}$, and $\mathbf{f}^{ext} = [f_h, -f_e]^{\mathrm{T}}$ are the master-slave position vector, the force control input vector, and the external force vector. $\mathbf{M} = \mathrm{diag}(m_m, m_s)$ stands for the mass matrix. The physical master-slave coordinates can be expressed in the new coordinates of position and force by the

use of the Hadamard matrix of second order $\mathbf{H}_2$ as the transformation matrix (note that $\mathbf{H}_2^T = \mathbf{H}_2$, $\mathbf{H}_2^{-1} = \frac{1}{2}\mathbf{H}_2$, $\mathbf{H}_2^2 = 2\mathbf{I}$).

$$\mathbf{H}_2 = \begin{bmatrix} 1 & 1 \\ 1 & -1 \end{bmatrix}. \tag{25}$$

It yields

$$\mathbf{y} = \mathbf{H}_2\mathbf{x} = \begin{bmatrix} 1 & 1 \\ 1 & -1 \end{bmatrix}\begin{bmatrix} x_m \\ x_s \end{bmatrix} = \begin{bmatrix} x_m + x_s \\ x_m - x_s \end{bmatrix}. \tag{26}$$

The equivalent dynamics in the virtual space

$$\mathbf{M}_y \ddot{\mathbf{y}} = \mathbf{f}_y + \mathbf{f}_y^{\text{ext}} \tag{27}$$

can be obtained such that by the transformation no power is generated and energy is preserved, *i.e.* $\dot{\mathbf{y}}^{\mathrm{T}}\mathbf{f}_y = \dot{\mathbf{x}}^{\mathrm{T}}\mathbf{f}$ and $\frac{1}{2}\dot{\mathbf{y}}^{\mathrm{T}}\mathbf{M}_y\dot{\mathbf{y}} = \frac{1}{2}\dot{\mathbf{x}}^{\mathrm{T}}\mathbf{M}\dot{\mathbf{x}}$:

$$\dot{\mathbf{y}}^{\mathrm{T}}\mathbf{f}_y = \dot{\mathbf{x}}^{\mathrm{T}}\mathbf{H}_2^{\mathrm{T}}\mathbf{f}_y = \dot{\mathbf{x}}^{\mathrm{T}}\mathbf{f} \quad \Rightarrow \quad \mathbf{f} = \mathbf{H}_2^{\mathrm{T}}\mathbf{f}_y. \tag{28}$$

Then the external forces in the virtual model can be expressed as:

$$\mathbf{f}_y^{\text{ext}} = \mathbf{H}_2^{-\mathrm{T}}\mathbf{f}^{\text{ext}} = \mathbf{H}_2^{-1}\mathbf{f}^{\text{ext}} = \frac{1}{2}\mathbf{H}_2\mathbf{f}^{\text{ext}}, \tag{29}$$

$$\mathbf{f}_y^{\text{ext}} = \begin{bmatrix} \dfrac{f_h - f_e}{2} & \dfrac{f_h + f_e}{2} \end{bmatrix}^{\mathrm{T}}. \tag{30}$$

The new coordinates are associated with the position error and the force error, respectively, and determine the virtual mode space of the bilateral teleoperation system (27). Note, that (27) implies $\dot{\mathbf{y}} = \mathbf{H}_2\dot{\mathbf{x}}$ and $\ddot{\mathbf{y}} = \mathbf{H}_2\ddot{\mathbf{x}}$. Hence, the teleoperator dynamics (24) can be now expressed by the new coordinates as

$$\mathbf{M}_y \ddot{\mathbf{y}} = \mathbf{f}_y + \mathbf{f}_y^{\text{ext}}, \tag{31}$$

where $\mathbf{M}_y$, $\mathbf{f}_y$ and $\mathbf{f}_y^{ext}$ represent the teleoperator mass matrix in the virtual modes, the virtual control input force, and the virtual external force; respectively, $\mathbf{f}_y = \frac{1}{2}\mathbf{H}_2\mathbf{f}$, $\mathbf{f}_y^{\text{ext}} = \frac{1}{2}\mathbf{H}_2\mathbf{f}^{\text{ext}}$. The mass matrix $\mathbf{M}_y$ can be obtained from the energy preservation requirement $\frac{1}{2}\dot{\mathbf{y}}^{\mathrm{T}}\mathbf{M}_y\dot{\mathbf{y}} = \frac{1}{2}\dot{\mathbf{x}}^{\mathrm{T}}\mathbf{M}\dot{\mathbf{x}}$. It follows

$$\frac{1}{2}\dot{\mathbf{y}}^{\mathrm{T}}\mathbf{M}_y\dot{\mathbf{y}} = \frac{1}{2}\dot{\mathbf{x}}^{\mathrm{T}}\mathbf{H}_2^{\mathrm{T}}\mathbf{M}_y\mathbf{H}_2\dot{\mathbf{x}} = \frac{1}{2}\dot{\mathbf{x}}^{\mathrm{T}}\mathbf{M}\dot{\mathbf{x}}, \tag{32}$$

$$\mathbf{M} = \mathbf{H}_2^{\mathrm{T}} \mathbf{M}_y \mathbf{H}_2 \quad \Rightarrow \quad \mathbf{M}_y = \mathbf{H}_2^{-\mathrm{T}} \mathbf{M} \mathbf{H}_2^{-1}. \tag{33}$$

One can note that $\mathbf{M}_y^{-1} = \mathbf{H}_2 \mathbf{M}^{-1} \mathbf{H}_2^{\mathrm{T}}$.

The coordinate transformation (25) decuples force and position coordinates of the coupled master-slave teleoperator architecture such that force servoing can be regulated in the *common mode*, while position tracking can be regulated in the *differential mode*. If one denotes $\mathbf{y} = \left[y_c, y_d \right]^{\mathrm{T}}$, then the common mode is assigned by the y_c coordinate, while the differential mode is assigned by the y_d coordinate, i.e. $y_c = x_m + x_s$ and $y_d = x_m - x_s$.

The impedance control offers a unified approach for the regulation in both position and force coordinates, and thus it may be applied to improve robot stability while contacting stiff environment. When the contact occurs, the arising forces will be dictated by the dynamic interbalancing of the system incorporating the human operator, the master and slave robot and the environment. To assign a prescribed dynamic behavior for the robot while its end-effector is interacting with the environment, the impedance control can be utilized to assure stable contact. It enables for controlling the robot in both free space and constrained motion control. A fundamental work on impedance control was published by [15]. The impedance control in bilateral telemanipulation has been introduced by [16]. Not necessarily, but normally 4-ch teleoperation paradigm is to be applied in fully impedance control [17].

In this paper, we prescribe the desired impedance of second order for the teleoperator system described in the virtual mode coordinates (34):

$$\mathbf{M}_y^d \ddot{\mathbf{y}} + \mathbf{B}_y^d \dot{\mathbf{y}} + \mathbf{K}_y^d \mathbf{y} = \mathbf{f}_y^{\mathrm{ext}}, \tag{34}$$

where $\mathbf{M}_y^d, \mathbf{B}_y^d, \mathbf{K}_y^d$ are the desired mass matrix, the desired damping matrix and the desired stiffness matrix in the virtual space, respectively, that can be arbitrary selected. $\mathbf{f}_y^{\mathrm{ext}}$ is the vector of external forces in the virtual space $\mathbf{f}_y^{\mathrm{ext}} = \mathbf{H}_2 \mathbf{f}^{\mathrm{ext}}$. It can be shown that if one chooses the desired impedance parameters such that $\mathbf{B}_y^d = \mathbf{M}_y^d \mathbf{K}_v$, $\mathbf{K}_y^d = \mathbf{M}_y^d \mathbf{K}_p$, furthermore selects $\mathbf{M}_y^d = \mathrm{diag}(M_c, M_d)$ with $0 < M_c < \infty$, $M_d \to \infty$, and the matrices of velocity and position feedback gains in the virtual modes are selected as $\mathbf{K}_v = \mathrm{diag}(0, k_v)$ and $\mathbf{K}_p = \mathrm{diag}(0, k_p)$, respectively, then the bilateral operation system dynamics can be expressed in the virtual modes as:

$$\ddot{y}_d + k_v \dot{y}_d + k_p y_d = 0, \tag{35}$$

$$M_c \ddot{y}_c = f_h - f_e . \tag{36}$$

Equations (35) and (36) decouple the force and position coordinates and furthermore determine optimally transparent and asymptotically stable bilateral teleoperation. Hence, in this paper they are assumed as control objective for the teleoperation system under consideration.

3. SLIDING MODE CONTROL DESIGN

The master and slave device of the teleoperator are robotic systems that can be viewed as multi-link mechanisms with revolute or prismatic joints. Such a robotic mechanism is represented by the highly nonlinear and intercoupled motion dynamics. Furthermore, a system model perturbation and external disturbance should be also considered within the control design. In this paper, the control design shall be performed in order to robustly decouple and linearize robot dynamics and to ensure the bilateral teleoperation given by the control objective in (35) and (36). In order to avoid undesired chattering, derivation of smooth control signal is prioritized.

3.1. CHATTERING-FREE SLIDING MODE CONTROL

Robotic manipulator mechanisms are generally characterized by multivariable input-output nonlinear dynamics and present a hard control problem. Centralized model-based control techniques can be applied in order to linearize behavior. An inverse dynamics calculation requires the complete knowledge of the robot dynamics. Consequently, such model-based control law techniques are sensitive to the structured and unstructured uncertainties, which always exist in the robot model, and the desired performance cannot be achieved. An alternative can be a robust decentralized approach in which only a single joint axis measurement is utilized in the independent joint controllers. Theory of Variable System Structure (VSS) provides a framework for Sliding Mode Control (SMC) that can be used for systems with bounded control input if the uncertainties in the model structure are bounded In this case, full disturbance rejection is possible if so-called matching condition is fulfilled. SMC guarantee robustness to system perturbations and external disturbance.

The system (9) can be abstracted by the following state space form:

$$\begin{aligned} \dot{z}_j &= z_{j+1} \\ \dot{z}_n &= f(\mathbf{z}) + b(\mathbf{z})u - d \end{aligned}, \tag{37}$$

where $j=1,...,n-1$, $\mathbf{z}=\left[z_1,...,z_n\right]^T$, u is scalar input, and $f(\mathbf{z})$, $b(\mathbf{z})$ are in general nonlinear functions of state. In the SMC approach, the goal of the control design is to find such control input u that restricts the motion of the system states $\mathbf{z}$ to a selected sliding manifold $\sigma(\mathbf{z},t)=0$. Here, $\sigma(\mathbf{z},t)$ is so called switching function that can be often selected as a linear combination of system states and time-variant reference, i.e. $\sigma(\mathbf{z},t)=r(t)-\mathbf{g}^{\mathrm{T}}\mathbf{z}$. It has been proven that control with discontinuities on the sliding manifold $\sigma(\mathbf{z},t)=0$:

$$u=\begin{cases}u^+, & \sigma(\mathbf{z},t)>0\\ u^-, & \sigma(\mathbf{z},t)<0\end{cases} \tag{38}$$

can enforce sliding mode if u^+ and u^- are selected such that the derivative of Lyapunov function candidate $v=\sigma^2/2$ is negative definite. By application of the equivalent control method u^+ and u^- can be selected such that $u^+>u_{\mathrm{eq}}>u^-$ are continuous functions of the system states and the equivalent control u_{eq} is solution of $\dot{\sigma}\big|_{\sigma=0}=0$. The dynamics of the closed loop system in the sliding mode are fully rejecting model perturbations and disturbances if the matching conditions are fulfilled. The SMC also reduces the order of the closed loop system. However, the discontinuous control has disadvantages related to the bang-bang control action that in mechanical systems may be hard to realize since forces are continuous function, and in addition it may excite high frequency dynamical terms. Therefore, such discontinues control must be strictly avoided in mechanical systems, since it causes well known chattering that may lead to increased wear of the actuators and to excitation of the high order unmodeled dynamics which can cause damage on mechanical parts and break the servo system.

A smooth control signal solution can be found by augmenting the original system with an additional system state in order to eliminate discontinuities on the control signal. It yields

$$\begin{aligned}\dot{z}_j&=z_{j+1},\\ \dot{z}_{n+1}&=h(\mathbf{z},u)+b(\mathbf{z})\dot{u}-\dot{d},\end{aligned} \tag{39}$$

where $h(\mathbf{z},u)=\dot{f}(\mathbf{z})+\dot{b}(\mathbf{z})u$, $\mathbf{z}=\left[z_1,\ldots,z_n\right]^{\mathrm{T}}$, and $j=1,...,n$. The derivative of v can have the form of $\dot{v}=-D\sigma^2$, where $D>0$ is arbitrary chosen control gain, which guarantees asymptotical reaching law. The switching function may have the form of $\sigma(\mathbf{z},t)=r(t)-(z_{n+1}+\mathbf{g}^{\mathrm{T}}\mathbf{z})$. From condition $\sigma\dot{\sigma}=-D\sigma^2$ and by application of the equivalent control method one can derive control u

$$u = \int_0^t \dot{u}\,\mathrm{d}\upsilon, \quad \dot{u} = \dot{u}_{eq} + D\sigma\,, \tag{40}$$

that assures an invariant system motion in the sliding mode. The system is said to be robust to the system perturbation and external disturbance that comply with the matching conditions.

The derivation of the continues sliding mode control law applies calculation of the equivalent control signal that requires complete information about systems dynamics, which is hardly to be exactly known in practice and thus it is not practical for implementation. Hence, the equivalent control signal is replaced with its estimated value which utilizes a nominal model and the rest is considered unknown system perturbation and disturbance. Thus, the control is implemented by

$$u = \hat{u}_{eq} + D\int_0^t \sigma\,\mathrm{d}\upsilon\,. \tag{41}$$

The control law has two components. One is representing estimation of the equivalent control which is based on the available model knowledge that is worthless to be neglected. Another can be referred to as a robust controller that is representing the disturbance estimation and the convergence to the selected sliding mode manifold. The block diagram of the SMC with smooth chattering-free control is shown by Fig. 3.

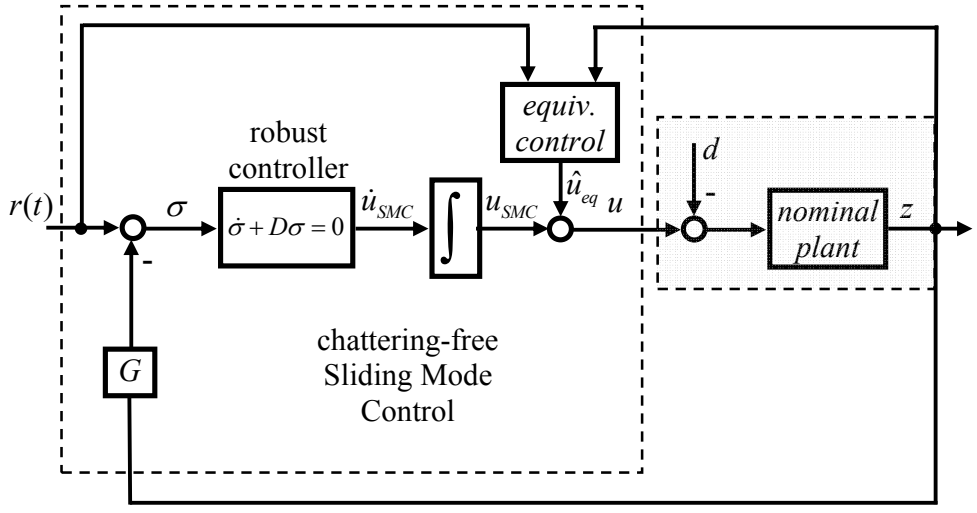

Fig. 3 – SMC block scheme.

The application of the Lyapunov function analysis shows that $\dot{v} = -D\sigma^2 - \sigma\dot{d}$. In order to guarantee invariant asymptotically stable solution $\sigma = 0$ the disturbance should satisfy the requirement $\dot{d} = 0$, or in other words, it should be constant. However, if disturbance changes relatively slowly, then $\dot{d} \approx 0$, and by high gain *D* can keep the system states in the vicinity of the sliding mode manifold ($\sigma \approx 0$). By proper tuning of *D* one can desensitize the system from the disturbance. Obviously, in steady state zero control error is assured. Thus, it is possible to satisfy control requirements given by the definition of the switching function and simultaneously perform smooth and fair robust control.

3.2. ROBUST BILATERAL CONTROL LAW DERIVATION

The SMC design procedure can be used for robust bilateral control. The first step in the derivation of SMC is to select sliding manifold on which the desired system dynamics will be enforced and thus one should define the switching function. Though, the master-slave system is evidently MIMO system, as shown above, it is possible to design two independent controllers for the master and the slave, respectively, and to ensure stability of the overall system. However, in this paper, the bilateral SMC design is applied by the definition of two switching functions formed on the basis of the virtual differential and common modes dynamics (25) in order to provide an independent force and position coordinate control. It yields two switching functions

$$\sigma_c = (\ddot{x}_m + \ddot{x}_s) - \frac{f_h - f_e}{M_c}, \tag{42}$$

$$\sigma_d = (\ddot{x}_m - \ddot{x}_s) + k_v(\dot{x}_m - \dot{x}_s) + k_p(x_m - x_s), \tag{43}$$

where index *d* refers to the differential position coordinate and index *c* refers to the common force coordinate of the teleoperator interconnected system. Furthermore, if one defines vector $\boldsymbol{\sigma} = [\sigma_c, \sigma_d]^{\mathrm{T}}$, then the compact form of the switching functions definitions (42)-(43) reads

$$\boldsymbol{\sigma} = \ddot{\mathbf{y}} + \mathbf{K}_v\dot{\mathbf{y}} + \mathbf{K}_p\mathbf{y} - \mathbf{M}_y^{d-1}\mathbf{f}_y^{\mathrm{ext}}. \tag{44}$$

Following the SMC design procedure presented in the previous section one can derive the bilateral control law from the requirement $\dot{\boldsymbol{\sigma}} = -D\boldsymbol{\sigma}$, *i.e.*

$$\dot{\boldsymbol{\sigma}} = \frac{\mathrm{d}}{\mathrm{d}t}\left\{\ddot{\mathbf{y}} + \mathbf{K}_v\dot{\mathbf{y}} + \mathbf{K}_p\mathbf{y} - \mathbf{M}_y^{-1}\mathbf{f}_y^{\mathrm{ext}}\right\} = -D\boldsymbol{\sigma}. \tag{45}$$

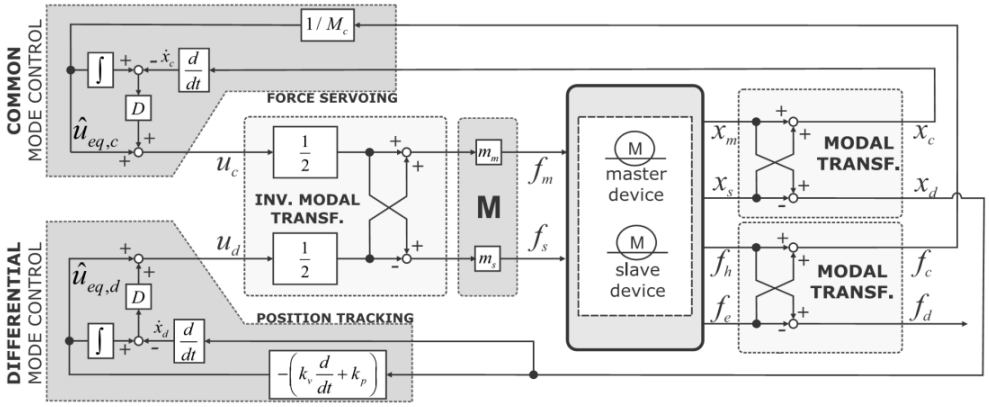

Fig. 4 – Robust bilateral control block scheme in the virtual modes.

From (45) one can express

$$\dot{\mathbf{u}} - \dot{\mathbf{u}}^{\text{dist}} + \frac{\mathrm{d}}{\mathrm{d}t}\left\{ \mathbf{K}_v \dot{\mathbf{y}} + \mathbf{K}_p \mathbf{y} - M_y^{d-1} \mathbf{f}_y^{\text{ext}} \right\} = -D\boldsymbol{\sigma}, \tag{46}$$

where $\mathbf{u} = \mathbf{M}_y^{-1}\mathbf{f}_y = \mathbf{H}_2\mathbf{M}^{-1}\mathbf{f}$, and $\mathbf{u}^{\text{dist}} = \mathbf{H}_2\mathbf{M}^{-1}(\mathbf{f}^{\text{dist}} - \mathbf{f}^{\text{ext}})$. Note that in this paper the disturbance signal $\mathbf{u}^{\text{dist}}$ involves also the effect of external force. It is meant to be fully rejected by internal control loop in order to decouple in and linearize the system in the virtual modes. The external force is natural negative feedback that could be compensated by measured force signal. However, such compensation signal may present a locally positive control feedback and thus can be a potential cause of instability. Furthermore, the use of force sensors may complicate the mechanical design. Therefore, as shown in the following, the external force shall be compensated asymptotically by control feedback based on motion signals.

In the sequence, by rearrangement and integration both sides of the equation (46) such that it results in the form $\mathbf{u} = \mathbf{u}_{\text{eq}} - D\int \boldsymbol{\sigma}\mathrm{d}t$, it yields

$$\mathbf{u} = \underbrace{\mathbf{u}^{\text{dist}} - \left\{ \mathbf{K}_v \dot{\mathbf{y}} + \mathbf{K}_p \mathbf{y} - M_y^{d-1} \mathbf{f}_y^{\text{ext}} \right\}}_{\mathbf{u}_{\text{eq}}} - \underbrace{\int D\boldsymbol{\sigma}\mathrm{d}t}_{\mathbf{u}_{\text{SMC}}}, \tag{47}$$

where $\mathbf{u}_{\text{eq}}$ is the equivalent control, and $\mathbf{u}_{\text{SMC}}$ is the robust control. Generally, the disturbance $\mathbf{u}^{\text{dist}}$ is considered as un-measurable signal. Hence, it is dropped from (47) and the *virtual mode control* in acceleration dimension can be written:

$$\mathbf{u} = \hat{\mathbf{u}}_{\text{eq}} - D\int \boldsymbol{\sigma}\,\mathrm{d}t\,, \tag{48}$$

where $\hat{\mathbf{u}}_{\text{eq}} = \mathbf{M}_y^{d-1}\mathbf{f}_y^{\text{ext}} - (\mathbf{K}_v\dot{\mathbf{y}} + \mathbf{K}_p\mathbf{y})$ is the estimation of the equivalent control. The control law (48) involves computation of the switching function $\boldsymbol{\sigma}$ that includes not only position $\mathbf{y}$ but also its velocity $\dot{\mathbf{y}}$ and acceleration $\ddot{\mathbf{y}}$, and the latter is non-measurable signal by assumption. However, it is possible to express $\int \boldsymbol{\sigma}\mathrm{d}t = \dot{\mathbf{y}} - \int \hat{\mathbf{u}}_{\text{eq}}\mathrm{d}t$ and the control law (48) turns to:

$$\mathbf{u} = \hat{\mathbf{u}}_{\text{eq}} + D(\int \hat{\mathbf{u}}_{\text{eq}}\mathrm{d}t - \dot{\mathbf{y}})\,. \tag{49}$$

If one denote $\mathbf{u} = \left[u_c, u_d\right]^{\mathrm{T}}$ and $\hat{\mathbf{u}}_{\text{eq}} = \left[\hat{u}_{\text{eq},c}, \hat{u}_{\text{eq},d}\right]^{\mathrm{T}}$ then the virtual control of the common and differential modes can be expressed in the component form:

$$u_c = \hat{u}_{\text{eq},c} + D(\int \hat{u}_{\text{eq},c}\mathrm{d}t - \dot{y}_c)\,, \tag{50}$$

$$u_d = \hat{u}_{\text{eq},d} + D(\int \hat{u}_{\text{eq},d}\mathrm{d}t - \dot{y}_d)\,, \tag{51}$$

where $\hat{u}_{\text{eq},c} = \dfrac{f_h - f_e}{M_c}$, and $\hat{u}_{\text{eq},d} = -(k_v\dot{y}_d + k_p y_d)$. Furthermore, it is easy to write the teleoperator control in the physical coordinate **f**:

$$\mathbf{f} = \mathbf{M}\mathbf{H}_2^{-1}\mathbf{u}\,. \tag{52}$$

The robust bilateral control scheme in the virtual modes is depicted by Figure 4.

3.3. REACTION FORCE OBSERVER

The bilateral controller described by equations (50)–(51) involves signals of contact forces both on master and slave sides. The force signal is conventionally obtained by force sensor, however, it can have poor dynamics characteristics and thus another solution may be sought for a vivid haptic sensation. The reaction force observer paradigm may be used for this purpose in order to provide fast force sensation response [14]. The reaction torque observer has been introduced in [27] following the well-known disturbance observer structure that is described by (53).

$$\hat{\tau}^{\text{dist}} = \frac{g}{s+g}\left(k_\tau i_a - gJ\omega\right) + gJ\omega\,. \tag{53}$$

Here, s stands for the complex variable in the so called complex s-plane, $\frac{g}{s+g}$ is a first order low-pass transfer function of the disturbance observer with the cut-off frequency g, that can be arbitrary chosen. J, k_τ, i_a, and ω are motor inertia, motor torque constant, motor armature current, and motor shaft velocity, respectively. The disturbance observer requires information of the shaft torque that is estimated by term $k_\tau i_a$. Modern servodrives implements fast and robust vector control, and consequently one can assume that the actual shaft torque follows the reference value that is calculated by speed or position tracking control algorithm. Thus, its output can replace the torque estimation in (53). However, following this concept, recently, external force observer has been introduced in the application of force control [14] and applied in various bilateral teleoperation control schemes [13, 28].

Considering the plant model given by (32), the observer of (re)action force on master and slave manipulator, respectively, can be described in time domain by a unique form (54),

$$\dot{\hat{f}}_j + g\hat{f}_j = g\left(f_i - gm_i \frac{\mathrm{d}}{\mathrm{d}t}\dot{x}_i\right) + gm_i \frac{\mathrm{d}}{\mathrm{d}t}\dot{x}_i, \tag{54}$$

where the indexes stand for $i = m,s$, and $j = h,e$. $\hat{f}_j$ is the observed signal of the actual external force. Such external force observer can be applied for (re)action force sensation and utilized in control law (50)–(51) instead of force sensors. It is easy to derive asymptotically stable estimation dynamics of such external force observer (55).

$$\dot{\hat{f}}_j + g\hat{f}_j = gf_j. \tag{55}$$

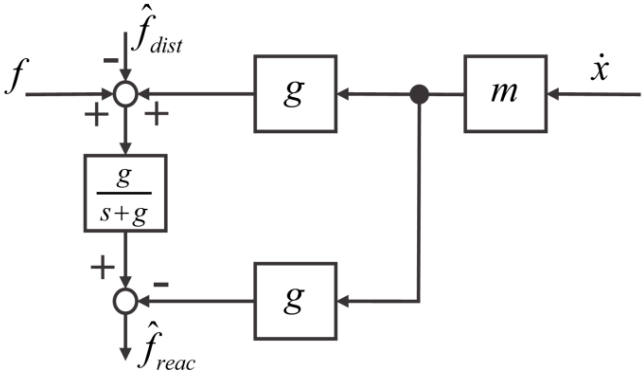

Fig. 5 – External force observer block scheme.

The proposed control law (50)-(51) involves the external force signals f_h and f_e, however, utilizing the force observer (54), (Figure 5) they can be replaced by their estimates $\hat{f}_h$ and $\hat{f}_e$. In order to analyze the effect of using the observer outputs instead of the actual signals one can express $\ddot{x}_m^c$ and $\ddot{x}_s^c$ by (56) and (57).

$$\ddot{x}_m^c = \ddot{x}_m - \frac{\sigma_f + \sigma_e}{2}, \tag{56}$$

$$\ddot{x}_s^c = \ddot{x}_s - \frac{\sigma_f - \sigma_e}{2}. \tag{57}$$

Here, the force signals are involved in the computation of σ_f. By the application of the force observers, σ_f involved in the control scheme consequently turns to $\hat{\sigma}_f$ such that one can notice the following relation:

$$\hat{\sigma}_f = \sigma_f + \frac{s}{s+g}\frac{f_h - f_e}{M_c}. \tag{58}$$

Without loss of generality regarding the further analysis one can assume $\mathbf{f}^{\text{dist}} = 0$. Then the application of the force observers leads to a change in the closed-loop dynamics such that (45) turns to

$$\dot{\hat{\sigma}}_f + D\hat{\sigma}_f = \frac{\dot{f}_h}{m_m} - \frac{\dot{f}_e}{m_s}. \tag{59}$$

By inserting expression (58) into (59) yields:

$$\dot{\sigma}_f + D\sigma_f = (1 - \frac{m_m}{M_c}\frac{s+D}{s+g})\frac{\dot{f}_h}{m_m} - (1 - \frac{m_s}{M_c}\frac{s+D}{s+g})\frac{\dot{f}_e}{m_s}. \tag{60}$$

In case of identical master and slave devices one can choose $M_c = m_m = m_s$ and $g = D$ that leads to the dynamics

$$\dot{\sigma}_f + D\sigma_f = 0, \tag{61}$$

where the right-hand side disappears.

4. THE EXPERIMENT

The efficiency of the proposed robust bilateral control scheme was validated by the experimental system shown in Figure 6. It consisted of two identical 1-DoF robot manipulators that comprise electrical linear motors. The motors can develop thrust forces f_m and f_s on master and slave side, respectively. They can move the

motor shafts with masses m_m and m_s, respectively. Each shaft can be used either to operate the system by a human on master side or to provide the environment contact on the slave side. A human operator can move the master motor shaft by force f_h. If the slave motor shaft established a contact with the environment, then the reaction force f_e occurs. The master-slave manipulator system includes Hall sensors that outputs voltages proportional to present magnetic field to measure the motor shaft position. The velocity was obtained by traditional discrete differentiation and filtering of the position signals. The external force information was estimated by the reaction force observer. The control system processed the data and output the analog voltage reference value to the servo drivers. The reference value presents the control force. The motor force was considered to be proportional to the motor current. The control algorithm was implemented by NI PXI-7841R with FPGA Virtex-5 [29]. Table 1 shows the manipulators parameters and the control parameters are shown in Table 2.

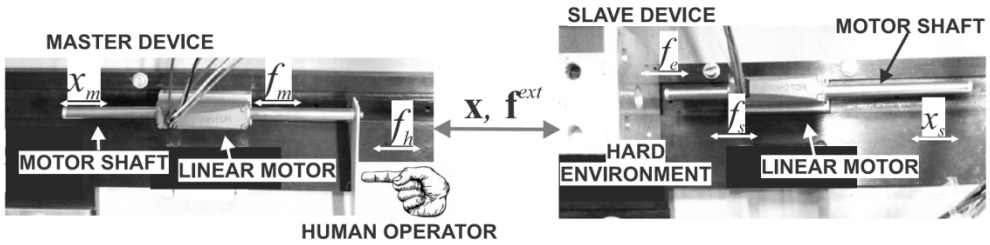

Fig. 6 – Experimental setup.

Experimental results are shown by Figure 7: a) free motion, b) contact with the soft environment, and c) contact with the hard environment. The diagrams depict position and force responses of the master system with solid line and the slave system with dashed line, respectively. In free motion only human operator holds the master shaft, while the slave shaft was unconstrained and followed the master motion command. Thus, only low operational force at the master handle was required. Almost perfect position tracking was observed. When the slave shaft was in contact (Fig. 7bc), simultaneous position and force tracking was observed. More specific, force tracking was almost perfect, whereas position tracking was slightly deteriorated.

Table 1

Master device maximum force $f_m^{\max}$	N	3.6
Slave device maximum force $f_s^{\max}$	N	3.6
Master device mass m_{m}	g	35
Slave device mass m_{s}	g	35

Table 2

Robustness disturbance D	1/s	250
Position gain k_p	$1/s^2$	12000
Velocity gain k_v	1/s	200
Virtual mass M_c	g	35
Control rate	kHz	50
Ext. force observer cutoff frequency g	rad/s	250
Velocity filter cutoff frequency f_0	rad/s	250

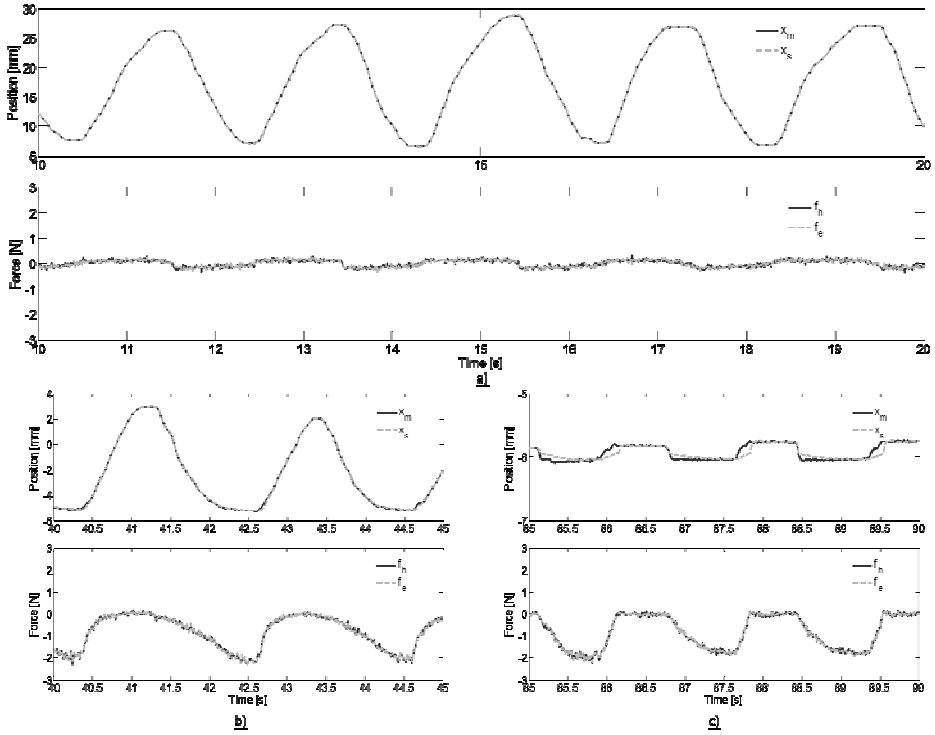

Fig. 7 – Experimental results for free motion (a), soft object contact (b), and hard object contact (c).

The experimental results show relatively low tracking error that only appeared due to relative poor quality of the velocity and external force signals. The bilateral teleoperation with vivid haptic interface requires high quality signals. Furthermore, the disturbance rejection capability of the bilateral control scheme is also strongly related to the values of the feedback gains – higher values provide stronger disturbance rejection and consequently better performance. High feedback gain D could be achieved only if high-quality measured signals with zero noise and

phase lag are obtained. Relatively noisy analog signals can be good enough for position measurement; however, it may not be good enough to obtain neither high quality velocity signal by the calculation scheme nor external force signal. The robustness could be also improved with higher values of the gain D of the robust controller; however, this is limited due to the noise/signal ratio of the measured signals and control rate. The proposed control scheme is significantly dependent on the quality of the velocity signal. Therefore the bilateral control performance could be improved by higher resolution of the measured signals. Extended experimental evaluation can be found in [30].

5. CONCLUSIONS

The paper presents a robust bilateral control scheme that was derived following the SMC design approach. The drawback of chattering that is well-known in the SMC theory was avoided, such that smooth continuous control has been derived that is required in motion control of mechatronic systems (when forces or torques are considered). The control scheme for bilateral teleoperation introduced virtual differential and common modes that decouple position and force coordinate. Desired impedance of second order is prescribed as control objective in the virtual space. High transparency required for haptic interface can be achieved for master and slave robots that can be of different configuration and mass inertia characteristics. The control scheme is simple and easy to implement with the potential to provide high robustness against the disturbance. Thus, it could be applied to achieve high-accuracy in robotic bilateral teleoperation applications with vivid haptic display. The proposed control scheme was experimentally validated for a 1-DoF master-slave teleoperator. The experiments showed that beside precise mechanism, high quality of measurement signals and acceleration control are extremely important in achievement of high-performance haptic-based teleoperation. In the future, the experimental validation will be performed on a multi-DoF telerobotic system.

Acknowledgements. Operation part financed by the European Union, European Social Fund.

Received on December 6, 2012

REFERENCES

1. SHERIDAN, T.B., *Telerobotics*, Automatica, **25**, *4*, pp. 487-507, 1989.
2. HASHTRUDI-ZAAD, K., SALCUDEAN, S.E., *Analysis and Evaluation of Stability and Performance Robustness for Teleoperation Control Architectures*, Proceedings IEEE International Conference on Robotics and Automation, April 2000, pp. 3107-3113.

3. LAWRENCE, D.A., *Stability and Transparency in Bilateral Teleoperation*, IEEE Transactions on Robotics and Automation, **9**, *5*, pp. 624-637, 1993.
4. YOKOKOHJI, Y., YOSHIKAWA, T., *Bilateral Control of Master-Slave Manipulations for Ideal Kinesthetic Coupling – Formulation and Experiment*, IEEE Transactions on Robotics and Automation, **10**, *5*, pp. 605-620, 1994.
5. DANIEL, R.W., McAREE, P.R., *Fundamental limits of performance for force reflecting teleoperation*, The International Journal of Robotics Research, **17**, *8*, pp. 811-830, 1998.
6. HASHTRUDI-ZAAD, K., SALCUDEAN, S.E., *On the use of local force feedback for transparent teleoperation*, Proceedings IEEE International Conference on Robotics and Automation, Vol. 3, pp. 1863-1869, May 1999.
7. CHOPRA, N., SPONG, M.W., ORTEGA, R., BARABANOV, N.E., *On tracking performance in bilateral teleoperation*, IEEE Transactions on Robotics, **22**, pp. 861-865, 2006.
8. SUMIYOSHI, Y., OHNISHI, K., *The transformation of modified 4-channel architecture*, 8th IEEE International Workshop on Advanced Motion Control, 2004, pp. 211-216.
9. MOTOI, N., KUBO, R., SHIMONO, T., OHNISHI, K., *Bilateral Control with Different Inertia Based on Modal Decomposition*, 11th IEEE International Workshop on Advanced Motion Control, Nagaoka, Japan, 2010.
10. OHNISHI, K., SHIBATA, M., MURAKAMI, T., *Motion Control for Advanced Mechatronics*, IEEE/ASME Transaction on Mechatronichs, **1**, *1*, pp. 56–67, 1996.
11. MATSUMOTO, Y., KATSURA, S., OHNISHI, K., *An Analysis and Design of Bilateral Control Based on Disturbance Observer*, Proceedings of the 10th IEEE International Conference on Industrial Technology, 2003, pp. 802–807.
12. TSUJI, T., NATORI, K., OHNISHI, K., *A Controller Design Method of Bilateral Control System*, Proceedings on International Power Electronics and Motion Control Conference and Exposition (EPE-PEMC), Vol. 4, pp. 123-128, 2004.
13. OHNISHI, K., KATSURA, S., SHIMONO, T., *Motion Control for Real World Haptics*, IEEE Industrial Electronics Magazine, June 2010, pp. 16-19.
14. KATSURA, S., MATSUMOTO, Y., OHNISHI, K., *Modeling of Force Sensing and Validation of Disturbance Observer for Force Control*, IEEE Transactions on Industrial Electronics, **54**, *1*, pp. 530-538, 2007.
15. HOGAN, N., *Impedance Control: An Approach to Manipulation, Part I, II, III*, Journal of Dynamic Systems, Measurement, and Control, **107**, pp. 1-23, March 1985.
16. MOORE, C.L., KAZEROONI, H., *Bilateral Impedance Control for Telemanipulators*, Japan/USA Symposium on Flexible Automation, Vol. 1, ASME 1992.
17. CHENG, C-C., ZHAO, Y-J., *A Telerobotic Manipulator System with Impedance Control*, Proceedings of the IEEE International Conference on Control Applications, Munich, Germany, October 4-6, 2006, pp. 193-198.
18. FRISOLI, A., SOTGIU, E., AVIZZANO, C.A., CHECCACCI, D., BERGAMASCO, M., *Force-based impedance control of a haptic master system for teleoperation*, Sensor Review, **24**, *1*, pp. 42-50, 2004.
19. DO, N.D., NAMERIKAWA, T., *Four-channel force-reflecting teleoperation with impedance control*, International Journal Advanced Mechatronic Systems, **2**, *5/6*, pp. 318-329, 2010.
20. CHO, H.C., PARK, J.H., *Impedance control with variable damping for bilateral teleoperation under time delay*, JSME International Journal, Serial C, **48**, *4*, pp. 695-703, 2005.
21. ALFI, A., FARROKHI, M., *Force Reflecting Bilateral Control of Master–Slave Systems in Teleoperation*, Journal of Intelligent Robot Systems, **52**, pp. 209-232, 2008.
22. UTKIN, V.I., *Sliding Modes in Control and Optimization*, Springer-Verlag, Berlin, 1992.

23. HACE, A., JEZERNIK, K., URAN, S., *Robust Impedance Control*, Proceedings of IEEE Conference on Control Applications CCA'98, Trieste, pp. 583-587, 1998.
24. KHAN, S., SABANOVIĆ, A., NERGIZ, A.O., *Scaled Bilateral Teleoperation Using Discrete-Time Sliding-Mode Controller*, IEEE Transactions on Industrial Electronics, **56**, *9*, pp. 3609-3618, 2009.
25. SCHILLING, R.J., *Fundamentals of Robotics*, Analysis and Control, Prentice Hall International, 1990.
26. IIDA, W., OHNISHI, K., *Reproducibility and operationality in bilateral teleoperation*, 8th IEEE International Workshop on Advanced Motion Control, pp. 217-222, 2004.
27. MURAKAMI, T., YU, F., OHNISHI, K., *Torque sensorless control in multi degree-of-freedom manipulator*, IEEE Transactions on Industrial Electronics, **40**, pp. 259-265, 1993.
28. SHIMONO, T., KATSURA, S., OHNISHI, K., *Abstraction and reproduction of force sensation from real environment by bilateral control*, IEEE Transactions on Industrial Electronics, **54**, *2*, pp. 907-918, 2007.
29. National Instruments, NI PXI-7841R R Series Multifunction RIO with Virtex-5 LX30 FPGA, [online] http://www.ni.com.
30. HACE, A., FRANC, M., *Robust haptic teleoperation by FPGA*, 10th IFAC Symposium on Robot Control, 2012, pp. 361-366.